

Research Article

Effect of the Intensive Plasticizing Zone Design on the Effectiveness of Corotating Twin-Screw Extrusion

Emil Sasimowski  and Łukasz Majewski 

Lublin University of Technology, Mechanical Engineering Faculty, Department of Polymer Processing and Technology, ul. Nadbystrzycka 36, 20-618 Lublin, Poland

Correspondence should be addressed to Łukasz Majewski; l.majewski@pollub.pl

Received 5 July 2018; Revised 20 February 2019; Accepted 10 March 2019; Published 16 April 2019

Academic Editor: Anil K. Bhowmick

Copyright © 2019 Emil Sasimowski and Łukasz Majewski. This is an open access article distributed under the Creative Commons Attribution License, which permits unrestricted use, distribution, and reproduction in any medium, provided the original work is properly cited.

The aim of this study was to investigate the effect of a new intensive plasticizing and mixing screw zone design on the effectiveness of the corotating twin-screw extrusion process for talc-filled polypropylene. The study determined the effect of the angle between the trilobe kneading elements forming the intensive plasticizing and mixing zone of the screws, the screw rotational speed, and the polypropylene/talc filling ratio on the characteristics of the extrusion process in a corotating twin-screw extruder EHP-2x20. The paper describes the experimental design and obtained results as well as the developed empirical models for selected variables of the extrusion process.

1. Introduction

The use of unmodified polymers has become insufficient to meet market requirements in terms of design and economy. Due to attempts at reducing production costs and a growing demand for materials with specified and unprecedented properties, polymer modifications are becoming more and more common [1, 2]. The properties of polymers can be changed by chemical or physical modification, by introducing mineral or natural fillers into the polymer matrix [1–4].

Polymer composition preparation is an interdisciplinary problem. When selecting the filler and its mass content in the matrix, one must take account of factors from the fields of chemistry, polymer physicochemistry, mechanics, rheology, materials engineering, and machine design [1, 2, 5, 6]. The selection of right filler and its proportions leads to the desired changes in material properties. Polymer compositions are most widely used to improve properties such as impact strength, hardness, abrasiveness, tensile or bending strength, chemical resistance, temperature stability, flammability, and thermal and electrical conductivity. However, the use of fillers is a compromise. Usually, the improvement of some properties leads to the deterioration of others [1, 2, 5, 7, 8]. Apart from the type and content of filler, the properties of

obtained compositions also depend on the degree of filler dispersion, the structure of the polymer itself, and the nature of adhesive phenomena occurring in the polymer, as well as the choice of processing technology and the design features of a machine for material processing [7, 9–12].

Obtaining the desired effect of polymer physical modification depends on the right distribution of the filler in the polymer matrix. The most popular types of fillers used in polymer processing are talc, carbonates, wollastonite, kaolin, and mica, i.e., fine-grained mineral fillers which tend to form agglomerates decreasing the strength of finished products [1, 5, 13, 14]. When using these fillers, it is particularly important to ensure an adequate degree of dispersion in the polymer matrix. For this reason, polymer composites and compositions, especially those with a high filling ratio, are most often fabricated using corotating twin-screw extruders, as these machines are characterized by very high mixing efficiency. The effect of good distributive mixing is achieved due to a significant share of radial mixing between a pair of the meshing elements and the polymer flow between the screws [5, 13, 15–17].

A plasticizing system with a modular design allows for adjusting its geometrical features to the technological requirements and the properties of a material. One can

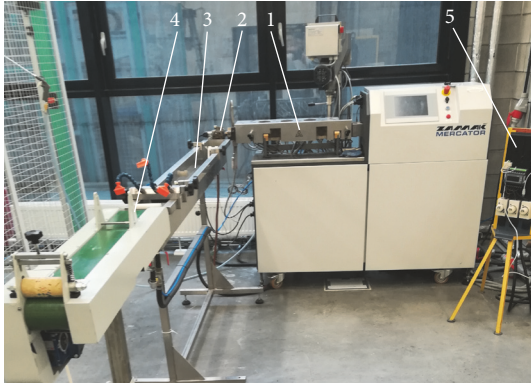


FIGURE 1: Test stand: 1, corotating twin-screw extruder; 2, extrusion head; 3, cooling tank; 4, belt puller; 5, electric energy meter.

distinguish several main types of elements of the processing screws: transporting, kneading, mixing, compressing, and expanding elements [18]. The design of the intensive mixing and plasticizing zone of the processing screws involves developing a given configuration of the kneading elements. The most popular kneading elements are two-lobe cams. They can be described with three basic parameters: the length, the angle of displacement of the cam elements relative to each other, and the thickness of the cam element [19]. The effect of the configuration of these parameters was of interest to many scientists already in the early 1990s [20–22]. The studies conducted at that time proved that the configuration of the kneading elements in the intensive mixing zone has a significant impact on the characteristics of the extrusion process. Results of a 2015 doctoral dissertation [23] report the effect of an additional parameter on the extrusion process, with this parameter being the distance between individual two-lobe cams forming the intensive mixing zone. On the other hand, the literature of the subjects lacks studies investigating the impact of such configuration in the intensive plasticizing and mixing zone composed of trilobe elements, especially in terms of their spacing, on the extrusion process and the properties of obtained extrudate.

The aim of this study was to investigate the effect of a new intensive plasticizing and mixing screw zone design on the effectiveness of the corotating twin-screw extrusion process for talc-filled polypropylene. The efficiency of the extrusion process is described using the output parameters, such as screw drive torque, a polymer melt pressure before the extrusion head, and a total electric power supplied to the extruder. Indirectly measured factors included a polymer mass flow rate, G [g/s], and a specific energy consumption of the extruder.

2. Experimental

2.1. Test Stand. Experiments were performed on a test stand (Figure 1) consisting of a corotating twin-screw extruder, EHP-2x20 Sline, from Zamak Mercator, provided with a plasticizing unit containing two modular screws with a diameter $D=20$ mm and an L/D ratio of 40, an extrusion

head with a 22.8 x 1.4 mm rectangular section nozzle for manufacturing polymer strips, a cooling tank, and a belt puller. The configuration of the processing screws and the test segment forming the intensive plasticizing and mixing zone is shown in Figure 2. The tested segment was composed of trilobe kneading elements, i.e., disk cams with a 10 mm width and transverse profile, as shown in Figure 3. The experiments were performed for 5 design solutions of the tested segment differing in terms of the angle between the interacting kneading elements, α , and the width of the gap between individual elements, d . The apparent helix inclination of successive lobes of the kneading elements was right-hand or neutral ($\alpha=0^\circ$). Every tested segment was located at a fixed distance from the extruder's feed opening.

2.2. Experimental Programme and Methods. The experiments were performed on polypropylene, Moplen EP440G, produced in the form of granules by LyondellBasell S.A. [24]. The filler was talc (hydrated magnesium silicate), Finntalc M15, manufactured by Mondo Minerals [25].

During the extrusion process, the temperature of nine heating zones of the barrel was maintained the same at 195°C ; the temperature of the connector and the extrusion head was also set to 195°C . This temperature value was selected on the basis of earlier studies on this problem [23, 26–28].

Prior to the extrusion process, polypropylene and talc were weighed in appropriate mass ratios and premixed before feeding them into the hopper. The extruder was gravity fed, and the PP/talc mixture level in the feed opening was maintained constant during extrusion.

Experiments were conducted in accordance with a full factorial design with two variables supplemented by the experiments in the centre of the plan. The ranges of independent variables (preset conditions of the process) applied in the experiments were as follows: the angle between the interacting kneading elements – $\alpha = 0\div 60^\circ$; the width of the gap between the kneading elements – $d = 0.5\div 4.5$ mm; the screw rotational speed – $n = 100\div 400$ min^{-1} ; and the filler mass fraction – $u=10\div 16$ %. The apparent helix inclination of successive lobes of the kneading elements was right-hand or neutral ($\alpha=0^\circ$).

The experimental tests involved direct measurements of the following variables: the measuring length mass of the extrudate m [g]; a screw drive torque, M [Nm]; a polymer melt pressure before the extrusion head, p [MPa]; and a total electric power supplied to the extruder, Q [kW] (consumed by the drive as well as the plasticizing and control units). Indirectly measured factors included a polymer mass flow rate, G [g/s], and a specific energy consumption of the extruder, E_{jc} [J/g]. The specific energy consumption E_{jc} was defined as a ratio of the total electric power supplied to the extruder Q and the polymer mass flow rate G . The above measures, M , p , G , E_{jc} , were dependent variables in the experiments. The adopted experimental design enabled the approximation of relationships between the dependent and independent variables by means of a multivariable polynomial consisting of linear polynomial terms as well as two-factor and three-factor interaction terms. Table 1 lists the experimental design

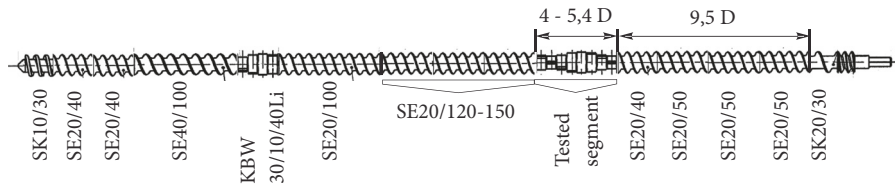


FIGURE 2: Configuration of the screws. SK represents single-flight transporting segments; SE represents double-flight transporting segments. The first number is the flight pitch, the second is the length of a segment, and KBW represents the kneading segments with double-lobe cams (disks). The first number is the angle between the cams' axes of symmetry, the second one is the width of cam elements, and the third is the length of a segment; the letter denotes the inclination of the apparent screw line of cam elements (Li: left; no letter: right).

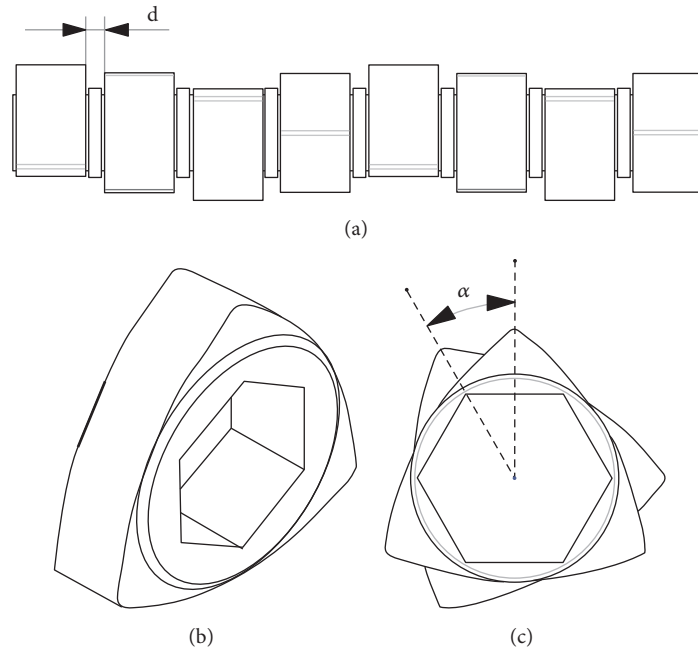


FIGURE 3: Schematic design of (a) tested segment, (b) three-lobe kneading element, (c) angle between the kneading elements, and (d) width of the gap between the kneading elements.

TABLE I: Experimental design.

Experimental design layout	$\alpha, ^\circ$	d, mm	n, min^{-1}	$u, \%$	M, Nm	p, MPa	$G, \text{g/s}$	$E_{ic}, \text{J/g}$
1	0	0.5	100	10	46.1	0.70	1.29	3182
2	0	0.5	100	16	43.2	0.82	1.34	3559
3	0	0.5	400	10	54.6	1.85	4.48	1832
4	0	0.5	400	16	48.1	1.80	4.29	1735
5	0	4.5	100	10	54.1	0.97	1.56	2665
6	0	4.5	100	16	39.7	0.82	1.20	3413
7	0	4.5	400	10	47.6	1.64	3.80	1847
8	0	4.5	400	16	43.8	1.75	3.89	1774
9	60	0.5	100	10	47.1	0.83	1.39	2785
10	60	0.5	100	16	43.1	0.93	1.36	3605
11	60	0.5	400	10	52.7	2.03	4.70	1669
12	60	0.5	400	16	41.7	1.71	3.58	1999
13	60	4.5	100	10	43.3	0.83	1.18	3377
14	60	4.5	100	16	38.6	0.77	1.14	4205
15	60	4.5	400	10	50.9	1.80	3.99	1790
16	60	4.5	400	16	50.1	1.86	4.11	1885
17 (C)	30	2.5	250	13	50.3	1.44	2.76	2055

TABLE 2: Analysis of variance results of the model of screw drive torque M , where the coefficient of determination is $R^2=0.93$ and its corrected value is $R_{adj}^2=0.91$. SS: sum of squares, df: number of the degrees of freedom, MS: mean sum of squares, F: values of the test statistic, p: value of probability corresponding to the test statistic value.

Source of variation	SS	df	MS	F	p
α	28.49	1	28.49	13.99	0.000373
d	22.27	1	22.27	10.93	0.001492
n	365.54	1	365.54	179.51	5.338755E-21
u	724.62	1	724.62	355.85	3.7173014E-29
αd	8.12	1	8.12	3.99	0.049687
αn	47.16	1	47.16	23.16	0.000008
αu	16.23	1	16.23	7.97	0.006190
dn	0.23	1	0.23	0.11	0.738255
du	0.21	1	0.21	0.10	0.751828
nu	4.87	1	4.87	2.39	0.126605
αdn	293.57	1	293.57	144.17	1.155914E-18
αdu	103.71	1	103.71	50.93	7.0363013E-10
αnu	29.63	1	29.63	14.55	0.000291
dnu	195.60	1	195.60	96.05	9.163506E-15
Error	142.54	70	2.04		
Total SS	1982.77	84			

TABLE 3: Analysis of variance results of the model of polymer pressure p , where the coefficient of determination and its corrected value are equal to $R^2 \approx R_{adj}^2=0.96$. SS: sum of squares, df: number of the degrees of freedom, MS: mean sum of squares, F: values of the test statistic, p: value of probability corresponding to the test statistic value.

Source of variation	SS	df	MS	F	p
α	0.05	1	0.05	5.35	0.023520
d	0.02	1	0.02	1.64	0.203922
n	18.83	1	18.83	1994.70	0.000000
u	0.01	1	0.01	1.13	0.292203
αd	0.02	1	0.02	2.13	0.148805
αn	0.03	1	0.03	3.31	0.072762
αu	0.02	1	0.02	2.48	0.119746
dn	0.06	1	0.06	6.66	0.011873
du	0.01	1	0.01	0.54	0.463822
nu	0.01	1	0.01	1.16	0.286015
Error	0.70	74	0.01		
Total SS	19.76	84			

layouts, according to which measurements were repeated five times.

3. Discussion of the Experimental Results

Obtained results of the study investigating the twin-screw extrusion process for talc-filled polypropylene are given in Table 1. The table lists the average values of the investigated dependent variables M , p , G , E_{jc} determined in individual layouts of the experimental design.

Based on measurement data, the regression coefficients of the empirical models describing the cause-and-effect

relationships between the dependent variables (subjected to observation) and a set of independent variables, i.e., preset conditions of the process, were determined.

The experimental results were statistically analysed by analysis of variance. Among others, the analysis involved verification of the elaborated empirical models and statistical evaluation of individual terms of the determined regression equations, the results of which are listed in Tables 2–5.

A Pareto chart of standardised effects was used to provide a statistically representative assessment of the impact of individual terms of the regression equations on the value of the modelled dependent variables. The vertical line in

TABLE 4: Analysis of variance results for the model of polymer mass flow rate G , with the coefficient of determination and its corrected version equal to $R^2 \approx R_{adj}^2=0.98$. SS: sum of squares, df: number of the degrees of freedom, MS: mean sum of squares, F: values of the test statistic, p: value of probability corresponding to the test statistic value.

Source of variation	SS	df	MS	F	p
α	0.048	1	0.05	1.11	0.295600
d	0.77	1	0.77	17.84	0.000067
n	156.59	1	156.59	3643.12	0.000000
u	0.69	1	0.69	16.01	0.000148
αd	0.04	1	0.04	0.92	0.340234
αn	0.02	1	0.02	0.43	0.512640
αu	0.13	1	0.13	3.07	0.084121
dn	0.28	1	0.28	6.53	0.012636
du	0.37	1	0.37	8.67	0.004322
nu	0.16	1	0.16	3.73	0.057367
Error	3.18	74	0.04		
Total SS	162.28	84			

TABLE 5: Analysis of variance results of the model of specific energy consumption of the extruder E_{jc} , where the coefficient of determination is equal to $R^2=0.92$ and its corrected value is $R_{adj}^2=0.90$. SS: sum of squares, df: number of the degrees of freedom, MS: mean sum of squares, F: values of the test statistic, p: value of probability corresponding to the test statistic value.

Source of variation	SS	df	MS	F	p
α	534847	1	534847	7.93	0.006214
d	109994	1	109994	1.63	0.205444
n	46964677	1	46964677	696.75	0.000000
u	2867537	1	2867537	42.54	7.534124E-9
αd	1021515	1	1021515	15.15	0.000215
αn	310571	1	310571	4.61	0.035110
αu	390014	1	390014	5.79	0.018653
dn	68935	1	68935	1.02	0.315178
du	8749	1	8749	0.13	0.719673
nu	1981075	1	1981075	29.39	0,000001
Error	4988010	74	67406		
Total SS	59245924	84			

the Pareto chart of standardised effects denotes the assumed significance level of $p = 0.05$, and the absolute values of the standardised effects exceeding this level are considered statistically significant.

3.1. Screw Drive Torque. The determined empirical model expressing the variability of the screw drive torque M as a function of four variables α , d , n , u is expressed by means of a polynomial in which, apart from the linear terms and two-factor interaction terms, three-factor interaction terms are also included.

$$\begin{aligned}
 M = & 43.1946 + 0.05122\alpha + 9.22153d + 0.0572997n \\
 & - 0.089291u - 0.130133\alpha d + 0.000225\alpha n \\
 & + 0.000460456\alpha u - 0.0291497dn - 0.615667du
 \end{aligned}$$

$$- 0.002443nu + 0.000213\alpha dn + 0.006325\alpha du$$

$$- 0.000045\alpha nu + 0.00174dnu$$

(1)

The necessity of considering three-factor interaction terms was prompted by the assessment of model fit carried out on the basis of the determination coefficient $R^2=0.93$ and its corrected value $R_{adj}^2=0.91$. When the three-factor interactions were not taken into account, these coefficients were equal to $R^2=0.61$ and $R_{adj}^2=0.56$, respectively.

Table 2 and Figures 4 and 5 present the results of modelling of the screw drive torque. The mass fraction of the filler u added to the processed polypropylene and the screw rotational speed n have the highest impact on the screw drive torque. One can also observe a significant influence (positive effect) of three-factor interactions, particularly between αdn ,

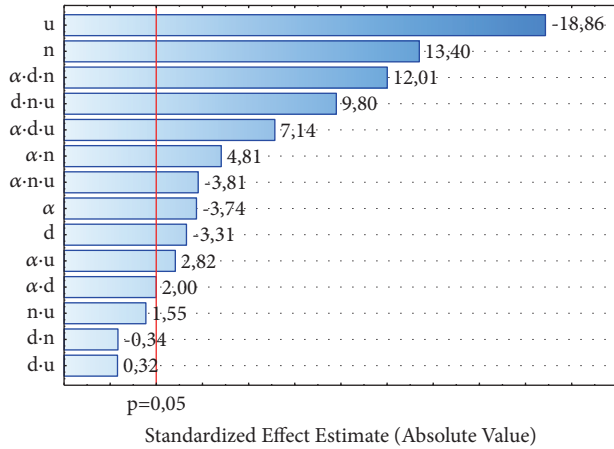


FIGURE 4: Pareto chart of standardised effects of the regression model of the screw drive torque M .

dna , and αdu as well as the interaction of αn . Increasing the talc content leads to a decrease in the screw drive torque. The highest decrease in the torque by 14.4 Nm (27%) due to increasing the talc content from 10% to 16% is observed between the comparable (with the same values of other independent variables) experimental design layouts 5 and 6. Increasing the talc content in the tested range causes a decrease in the viscosity of the PP/talc mixture, which is reflected, among others, in a significant increase in its mass flow rate, as demonstrated in studies [26, 29]. A similar effect of increased talc content on reducing the screw drive torque was observed in studies [23, 30]. On the other hand, increasing the screw rotational speed leads to an increase in the torque of the screw drive. This is due to a simultaneous increase in the polymer mass flow rate resulting from the use of the gravity feed extruder. The highest increase in the screw drive torque of 11.5 Nm (30%) occurs as a result of a four-time increase in the screw rotational speed between the comparable experimental layouts 14 and 16. Studies [23, 30] report a different effect of the screw rotational speed on the torque value because they used forced feeding of the extruder, which caused incomplete filling of the system with the plastic (polymer flow rates were constant).

3.2. Polymer Pressure. The dependence describing the variations in the polymer pressure p , measured before the extrusion head as a function of four variables α , d , n , u , is expressed by a polynomial with linear terms and two-factor interaction terms.

$$\begin{aligned}
 p = & 0.399454 + 0.002869\alpha + 0.006983d + 0.003674n \\
 & + 0.005011u - 0.000264\alpha d + 0.000004\alpha n \\
 & - 0.00019\alpha u - 0.000093dn + 0.001333du \\
 & - 0.000026nu
 \end{aligned} \quad (2)$$

Table 3 and Figures 6 and 7 present the results of a statistical analysis of the impact of extrusion conditions on

the pressure of the processed material. The screw rotational speed has the greatest impact on this variable. Increasing the screw rotational speed leads to a clear increase in the pressure of the polymer. This increase results from both a higher polymer flow rate and higher polymer viscosity due to a shorter residence time of the polymer in the plasticizing system. A four-time increase in the screw rotational speed causes the highest observed increase in the polymer pressure of 1.2 MPa between the comparable experimental layouts 9 and 11. The modelling results also indicate the presence of a statistically significant interaction between n and d (negative effect) and the influence of the angle α describing the position of the kneading element relative to each other. However, the impact of these factors is much lower. Also in this case, we can observe a different pattern of changes compared to that reported in studies [23, 30], among others, due to a different method of power supply to the extruder.

3.3. Polymer Flow Rate. An empirical model describing the dependence of the polymer mass flow rate G as a function of four variables α , d , n , u is represented by the following polynomial.

$$\begin{aligned}
 G = & 0.727308 + 0.00327\alpha - 0.158583d + 0.011012n \\
 & - 0.020965u + 0.000371\alpha d + 0.000003\alpha n \\
 & - 0.000451\alpha u - 0.000198dn + 0.011375du \\
 & - 0.000099nu
 \end{aligned} \quad (3)$$

The results of modelling of the polymer mass flow rate are presented in Table 4 and Figures 8 and 9. A significant relationship can be observed between the polymer mass flow rate G and the conditions of the extrusion process such as the screw rotational speed n , the gap width between the kneading elements d , and the talc mass fraction u . As in the case of the polymer pressure, the screw rotational speed has the greatest impact on the polymer mass flow rate, and increasing this variable causes a proportional increase in the flow rate of the polymer. The highest increase in the polymer flow rate amounting to 3.3 g/s was observed—similarly to the case of polymer pressure—between the experimental layouts 9 and 11. Increasing the gap width between the kneading elements d reduced the transport of the polymer in the tested segment and, consequently, also decreased the flow rate of the polymer. The highest decrease in the polymer mass flow rate by 0.7 g/s (15%) due to increasing the gap to $d=4.5$ mm was observed at the highest tested screw speeds, respectively, at $\alpha=0^\circ$ between the layouts 3 and 7 and at $\alpha=90^\circ$ between the layouts 11 and 15. The talc mass fraction u has a similar effect on the mass flow rate of the polymer. The interactions between du and dn factors are also statistically significant, although their impact is significantly lower.

3.4. Specific Energy Consumption. On the basis of results obtained from the measurements carried out according to the experimental design, an empirical model describing the

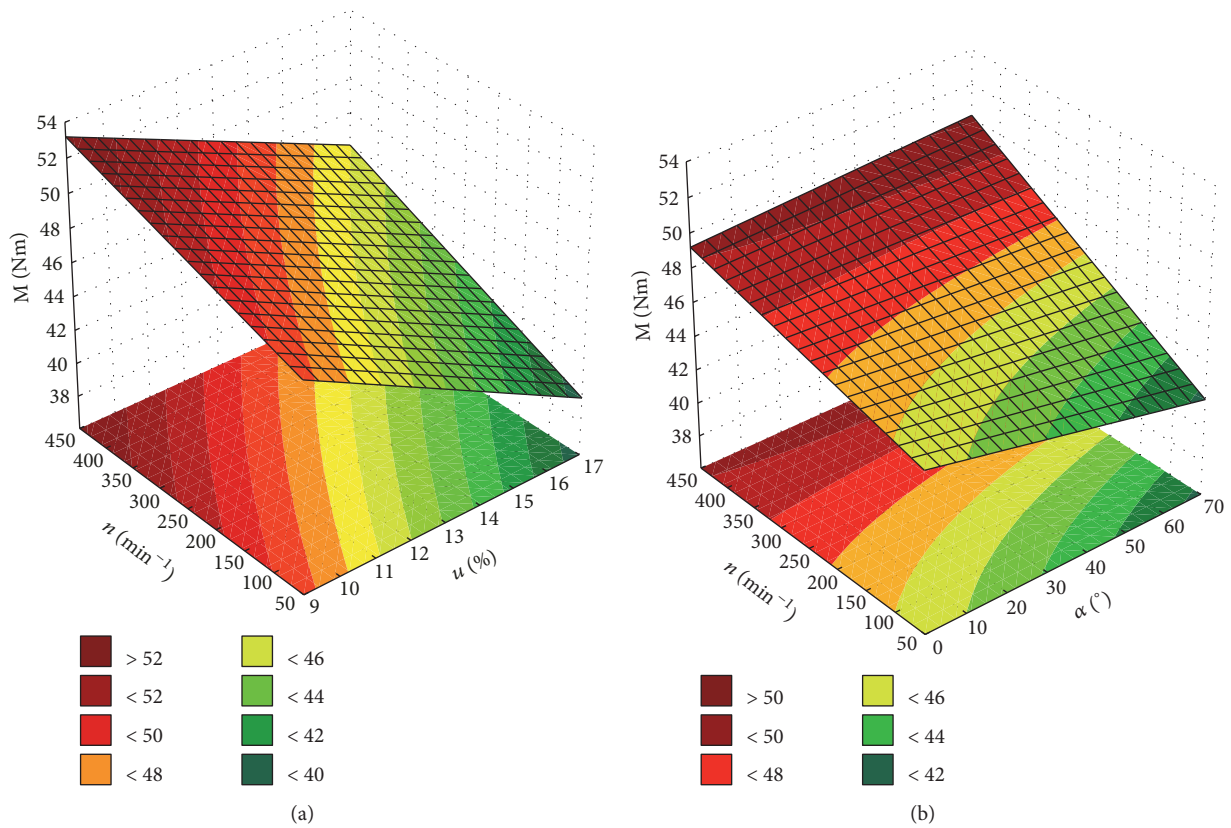


FIGURE 5: Model of the screw drive torque M , response surface versus the screw rotational speed n and (a) talc mass fraction u , (b) angle between the kneading elements α .

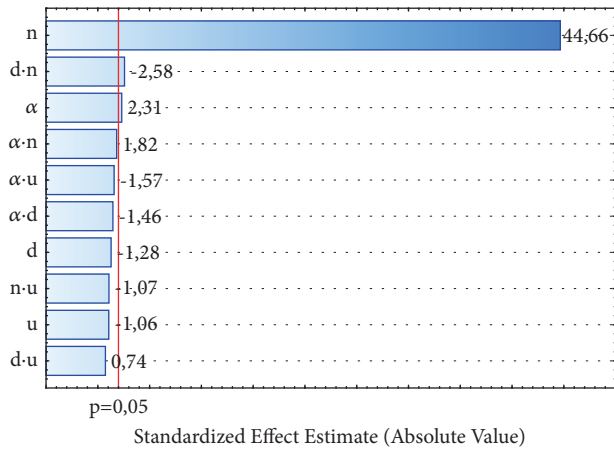


FIGURE 6: Pareto chart of standardised effects of the regression model of the polymer pressure p .

total specific energy consumption of the extruder E_{jc} was developed and expressed with the following polynomial.

$$E_{jc} = 2079.15 - 8.60678\alpha - 36.1557d + 0.098089n + 122.902u + 1.88333\alpha d - 0.013846\alpha n$$

$$+ 0.775805\alpha u - 0.097848dn + 1.74292du - 0.349698nu \quad (4)$$

Table 5 and Figure 10 present the results of statistical analysis of the impact of extrusion conditions on the specific energy consumption of the extruder.

As in the case of torque, the variables that have the greatest impact on this measure are the screw rotational speed n and the mass fraction of talc u added to the processed polypropylene. However, the nature of this impact is different. Increasing the rotational speed of the screws results in decreasing the specific energy consumption of the extruder. This is due to the fact that the increase in the polymer mass flow rate is higher than the increase in the energy supplied to the extruder. On increasing the screw rotational speed by four times, the highest decrease in the specific energy consumption of the extruder by 2320 J/g (55%) was observed between the comparable experimental layouts, 14 and 16.

Increasing the talc content leads to an increase in the specific energy consumption—this increase is particularly visible in the range of low screw speeds and it decreases with increasing their speed. This results from the confirmed interaction between these factors. As a result of increasing the talc content from 10% to 16%, the highest increases in specific

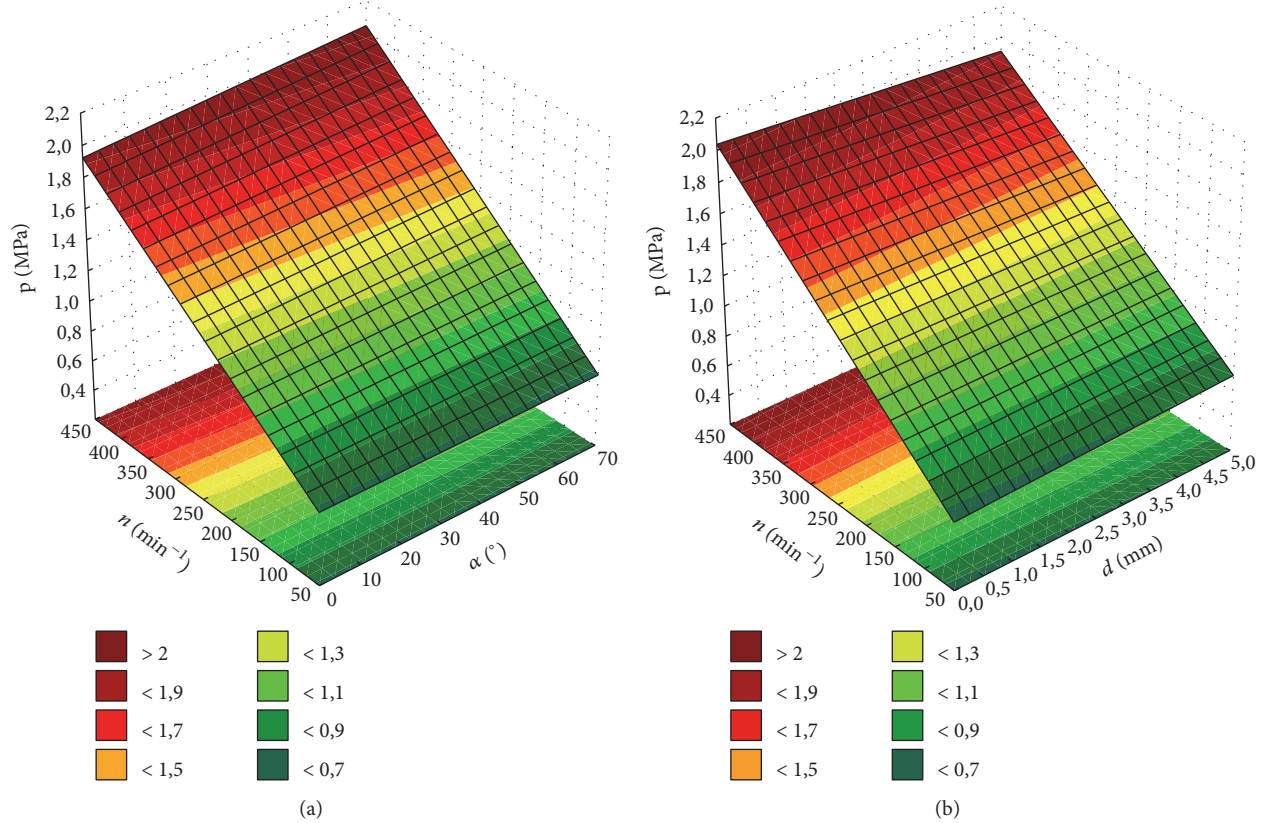


FIGURE 7: Model of the polymer pressure p , response surface versus the screw rotational speed n and (a) the angle between the kneading elements α , (b) width of the gap between the kneading elements d .

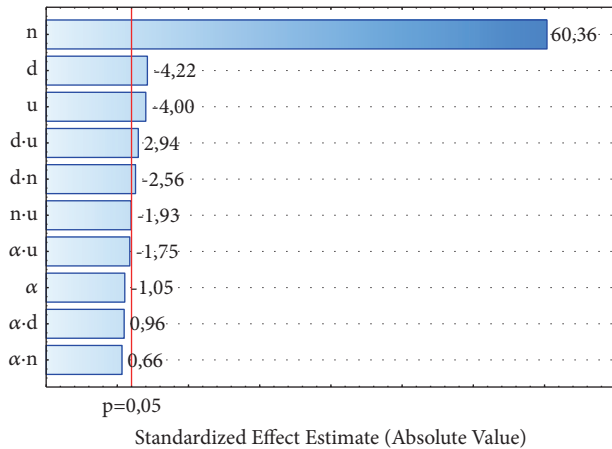


FIGURE 8: Pareto chart of standardised effects of the regression model of the polymer mass flow rate G .

energy consumption by 820 J/g (29%) and by 828 J/g (25%) were observed between the comparable experimental layouts: 9 and 10 and 13 and 14.

The modelling results also showed a significant influence of the angle between the kneading elements α and the presence of two statistically significant interactions between

ad and αu (positive effects). Figure 11 presents the changes in specific energy consumption as a function of the above factors.

4. Conclusion

Based on the obtained test results and the performed analyses, it can be concluded that the screw rotational speed has the greatest impact on the investigated extrusion process. A high screw rotational speed (in the tested range) has a positive effect on the polymer mass flow rate, the efficiency of the extrusion process, the pressure of the processed material, and the specific energy consumption of the extruder. However, high screw rotational speeds also cause a significant increase in the screw drive torque. As for the factors describing the tested segment of the processing screws, it has been found that both the gap width and the angle between the kneading elements are statistically significant for the extrusion process. The results reveal that, in most cases, the above factors interact with other investigated independent variables. Increasing the width of the gap between the kneading elements causes a decrease in the polymer pressure and its mass flow rate and, thus, leads to an increase in the specific energy consumption of the extruder. Increasing the angle between the kneading elements and, hence, the right-hand inclination of the apparent helix of the lobes of these elements also leads

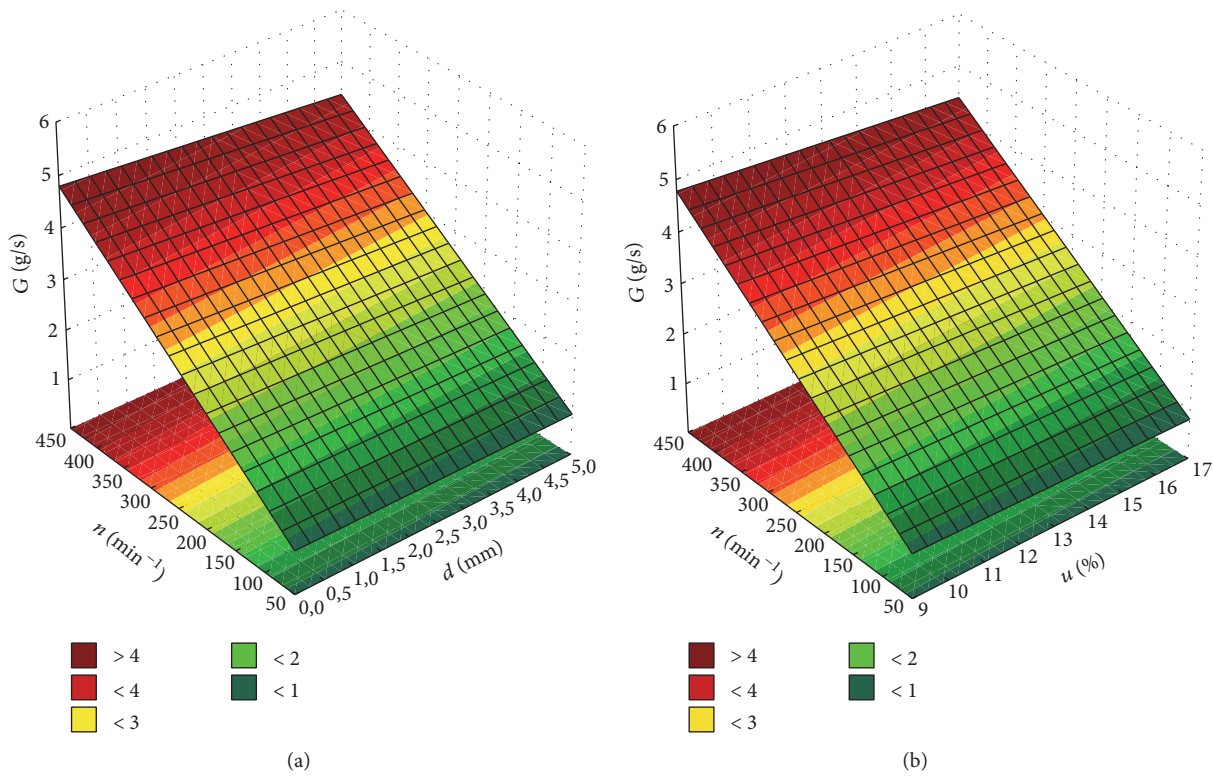


FIGURE 9: Model of the polymer mass flow rate G , response surface plots for the polymer mass flow rate G versus the screw rotational speed n and (a) width of the gap between the kneading elements d , (b) mass fraction of talc u .

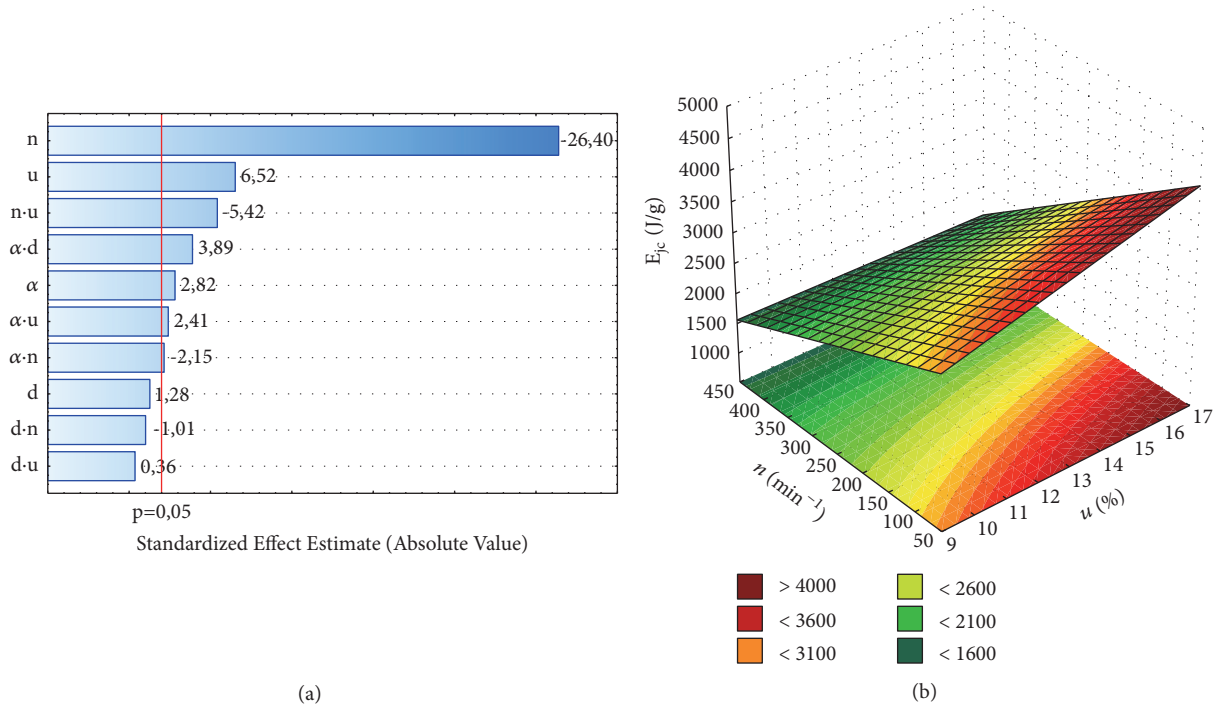


FIGURE 10: Model of specific energy consumption of the extruder E_{jc} . (a) Pareto chart of standardised effects of the regression model, (b) response surface versus the screw rotational speed n and the mass fraction of talc u .

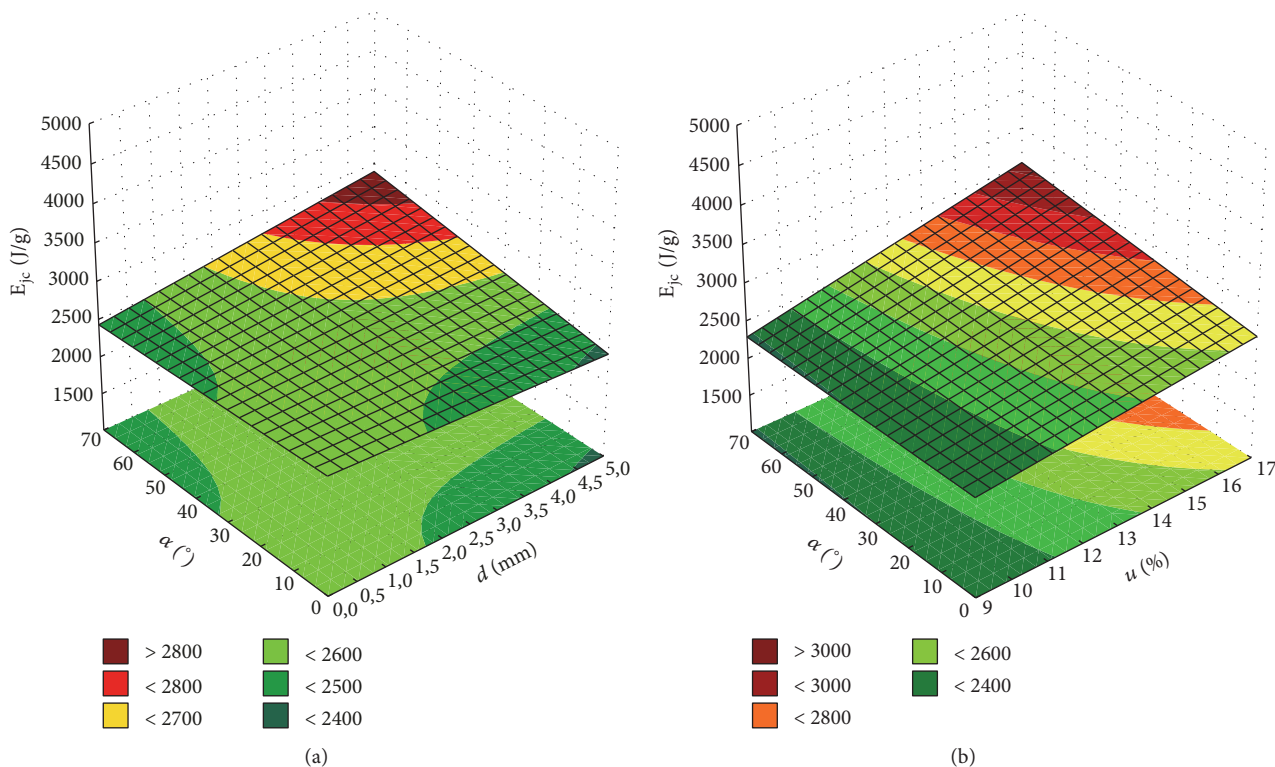


FIGURE 11: Response surface plots for the specific energy consumption of the extruder, E_{jc} , versus the angle between the kneading elements, α , and (a) width of the gap between the kneading elements, d , (b) mass fraction of talc, u .

to an increase in the specific energy consumption of the extruder and a slight increase in the pressure of the processed material. This, however, has not been found to be statistically significant for the polymer mass flow rate. The nature of impact on the screw drive torque depends on the interaction with other independent variables.

Increasing the mass fraction of talc-polypropylene filler in the tested range has a significant impact on decreasing the screw drive torque and the polymer mass flow rate and, thus, on increasing the specific energy consumption of the extruder. However, no significant impact of this variable on the polymer pressure has been observed.

Besides the description of the extrusion process presented in the paper, the properties of the extrudate obtained from this process are of significant importance for both cognitive and practical reasons. The effect of the applied design solutions of the tested segment of the processing screws on selected properties of the obtained extrudate will be the subject of a separate publication.

Data Availability

The data used to support the findings of this study are available from the corresponding author upon request.

Conflicts of Interest

The authors declare that there are no conflicts of interest regarding the publication of this paper.

References

- [1] M. Xanthos, *Functional Fillers for Plastics*, WILEY-VCH Verlag GmbH & Co. KGaA, Weinheim, Germany, 2010.
- [2] H. Katz and J. Milewski, *Handbook of fillers for plastics*, Van Nostrand Reinhold, New York, NY, USA, 1987.
- [3] A. Tor-Świątek, "Evaluation of the effectiveness of the micro-cellular extrusion process of low density polyethylene," *Maintenance and Reliability*, vol. 15, no. 3, pp. 225–229, 2013.
- [4] B. Samujło, "Characteristic of the extrusion of polyethylene modified with halogen free flame retardants and additives," *Polimery*, vol. 48, no. 7-8, pp. 540–544, 2003.
- [5] R. Rothon, *Particulate-Filled Polymer Composites*, Rapra Technology Limited, Shawbury, UK, 2nd edition, 2003.
- [6] J. W. Sikora and E. Sasimowski, "Influence of the length of the plasticating system on selected characteristics of an autothermal extrusion process," *Advances in Polymer Technology*, vol. 24, pp. 21–28, 2005.
- [7] R. Rothon, "Mineral fillers in thermoplastics: filler manufacture and characterisation," *Advances in Polymer Science*, vol. 139, pp. 67–107, 1999.
- [8] T. Chou, *Structure and Properties of Composites. Materials Science and Technology*, vol. 13, VCH Verlagsgesellschaft, Weinheim, Germany, 1993.
- [9] P. Mareri, S. Bastide, N. Binda, and A. Crespy, "Mechanical behaviour of polypropylene composites containing fine mineral filler: Effect of filler surface treatment," *Composite Science and Technology*, vol. 58, p. 747, 1998.
- [10] T. Klepka, R. Jeziórska, and A. Szadkowska, "Thin wali products made of modified high density polyethylene," *Przemysł Chemiczny*, vol. 94, no. 8, pp. 1352–1355, 2015.

- [11] E. Sasimowski, "Studies in the effectiveness of a new generation extruder. Part IV. The comparison of performance of the extruder model with its prototype," *Polimery*, vol. 58, no. 7-8, pp. 597–604, 2013.
- [12] E. Sasimowski, "Studies in the effectiveness of a new generation extruder. Part I. The influence of the location of the rotating sleeve of the barrel in the plasticizing system," *Polimery*, vol. 56, no. 5, pp. 390–396, 2011.
- [13] H. Karian, *Handbook of Polypropylene and Polypropylene composites, Revised and Expanded*, CRC Press, Boca Raton, Fla, USA, 2003.
- [14] T. Jachowicz and L. Dulebova, "Study on the effects of mineral filler content on the p-v-T characteristics of polypropylene," *Przemysł Chemiczny*, vol. 12, p. 2295, 2015.
- [15] J. Stasiak, "The Influence of Fillers and Process Conditions of Co-rotating Twin-screw Extrusion on Composite Properties, APT'03," Katowice, 2003.
- [16] J. L. White and H. Potente, *Screw Extrusion, Science and Technology*, Hanser Publishers, Munich, Germany, 2003.
- [17] T. Sakai, "Screw extrusion technology - Past, present and future," *Polimery*, vol. 58, pp. 847–857, 2013.
- [18] J. Stasiak and J. Gołębiewski, "The properties of inorganic filled polypropylene resin composites as affected by the co-rotating twin-screw extrusion conditions," *Przemysł Chemiczny*, vol. 82, p. 962, 2003.
- [19] C. Rauwendaal, *Mixing in Polymer Processing*, Marcel Dekker Inc, New York, NY, USA, 1991.
- [20] J. L. White, S. Montes, and J. M. Kim, "Experimental study and practical engineering analysis of flow mechanisms and starvation in a modular intermeshing corotating twin screw extruder," *Kautschuk und Gummi, Kunststoffe*, vol. 43, no. 1, pp. 20–25, 1990.
- [21] J. L. White and Z. Chen, "Simulation of non-isothermal flow in modular co-rotating twin screw extrusion," *Polymer Engineering Science*, vol. 34, no. 3, pp. 229–237, 1994.
- [22] M. A. Huneault, M. F. Champagne, and A. Luciani, "International forum on polymers—1995: Part I," *Polymer Engineering & Science*, vol. 36, no. 2, pp. 161-162, 1996.
- [23] A. Stasiak, University of Science and Technology, Bydgoszcz, Poland, 2015.
- [24] 2018, http://www.basellorlen.pl/assets/produkty/produkty/Moplen_EP440G_201410_PL.pdf.
- [25] 2018, http://www.mondominerals.com/product-details/?tx_drivermondoproducts_pil%5Bitem%5D=25&cHash=fc248dd5ad8-a74129206aef20eb01e0d.
- [26] J. Stasiak, "The effects of constructional solutions of plasticizing screw configurations and extrusion conditions on polypropylene composite properties," *Polimery*, vol. 50, pp. 881–889, 2005.
- [27] J. Stasiak, K. Bajer, A. Stasiak, and M. Bogucki, "Co-rotation twin-screw extruders for polymer materials. A method for experimental studying the extrusion process," *Przemysł Chemiczny*, vol. 91, no. 2, pp. 224–230, 2012.
- [28] J. Stasiak, "Polish Patent PL207893," 2011.
- [29] A. Stasiak and D. Łubkowski, "Investigations of the influence of construction of segments of the screws of co-rotating twin-screw extruders and technological parameters on the extrusion process of polypropylene modified with talc," *Przetwórstwo Tworzyw*, vol. 16, p. 8, 2010.
- [30] A. Stasiak, D. Łubkowski, and M. Bogucki, "Study on extrusion of talc-filled polypropylene," *Przemysł Chemiczny*, vol. 91, no. 8, pp. 1625–1629, 2012.



Hindawi
Submit your manuscripts at
www.hindawi.com

